THE JOURNAL OF BIOLOGICAL CHEMISTRY
Vol. 272, No. 14, Issue of April 4, pp. 8946–8956, 1997

Printed in U.S.A.

Demonstration of Coiled-Coil Interactions within the Kinesin Neck Region Using Synthetic Peptides

IMPLICATIONS FOR MOTOR ACTIVITY*

(Received for publication, December 4, 1996, and in revised form, January 15, 1997)

Brian Tripet‡§, Ronald D. Vale¶, and Robert S. Hodges‡§‖

From the ‡Department of Biochemistry and the §Medical Research Council Group in Protein Structure and Function, University of Alberta, Edmonton, Alberta T6G 2H7, Canada and the ¶Howard Hughes Medical Institute and Departments of Pharmacology and Biochemistry/Biophysics, University of California, San Francisco, California 94143

Kinesin is a dimeric motor protein that can move for several micrometers along a microtubule without dissociating. The two kinesin motor domains are thought to move processively by operating in a hand-over-hand manner, although the mechanism of such cooperativity is unknown. Recently, a ~50-amino acid region adjacent to the globular motor domain (termed the neck) has been shown to be sufficient for conferring dimerization and processive movement. Based upon its amino acid sequence, the neck is proposed to dimerize through a coiled-coil interaction. To determine the accuracy of this prediction and to investigate the possible function of the neck region in motor activity, we have prepared a series of synthetic peptides corresponding to different regions of the human kinesin neck (residues 316–383) and analyzed each peptide for its respective secondary structure content and stability. Results of our study show that a peptide containing residues 330–369 displays all of the characteristics of a stable, two-stranded α-helical coiled-coil. On the other hand, the NH_2-terminal segment of the neck (residues ~316–330) has the capacity to adopt a β-sheet secondary structure. The COOH-terminal residues of the neck region (residues 370–383) are not α-helical, nor do they contribute significantly to the overall stability of the coiled-coil, suggesting that these residues mark the beginning of a hinge located between the neck and the extended α-helical coiled coil stalk domain. Interestingly, the two central heptads of the coiled-coil segment in the neck contain conserved, "non-ideal" residues located within the hydrophobic core, which we show destabilize the coiled-coil interaction. These residues may enable a portion of the coiled-coil to unwind during the mechanochemical cycle, and we present a model in which such a phenomenon plays an important role in kinesin motility.

Understanding how motor proteins generate force and movement from the chemical hydrolysis of ATP remains one of the most intriguing problems in biophysics. At present, there are three separate families of motor proteins found within eukaryotic cells: myosins, which move along actin filaments, and kinesins and dyneins, which move along microtubules (1). The motor domains that typify each of these superfamilies exhibit little or no amino acid sequence similarity, and hence it was believed that they had evolved separately and were structurally unrelated. However, the recently determined crystal structure of kinesin revealed an unexpected structural similarity to the core of the myosin motor domain, particularly in the nucleotide binding pocket (2, 3). Hence, myosin and kinesin may share some similarities in how they generate unidirectional movement and force, although the precise mechanistic details remain to be elucidated for both types of motors.

Kinesin has proven to be an excellent model system for investigating the mechanism of motility, in part due to the small size of its motor domain (>2-fold smaller than myosin's). Kinesin purified from tissue sources exists as an $\alpha_2\beta_2$ heterotetramer, in which two α subunits (heavy chains) and two β subunits (light chains) associate to form a highly elongated molecule with globular termini (4, 5). The kinesin heavy chains are organized into four domains (listed from NH_2 to COOH terminus): (i) a ~325-amino acid residue globular motor domain head that contains the ATP and microtubule binding sites, (ii) a ~50-amino acid residue region adjacent to the globular motor domain (termed the neck region) that is sufficient for allowing dimerization of the motor domains (6) and contains a sequence that is predicted to form an α-helical coiled coil (6, 7), (iii) a long (~450-amino acid residue) α-helical coiled-coil domain (termed the stalk), and (iv) a small globular COOH terminus (termed the tail) (8–11). Flexible "hinge" regions are found between the neck and the stalk and in the center of the stalk. The light chains (β subunits) of kinesin, which are not necessary for force-generation, are associated with the smaller globular COOH terminus of the heavy chain and may be involved in determining cargo specificity (8).

A single kinesin molecule can move continuously along a microtubule for several micrometers in a series of 8-nm steps, which corresponds to the distance between tubulin binding sites along the microtubule protofilament (12). Such processive movement, which is not displayed by muscle myosin or ciliary dynein, very likely represents a specialized adaptation that enables a few kinesin motors to transport membrane organelles efficiently within cells. Functional studies on recombinantly expressed kinesin heavy chains have begun to uncover regions that are necessary for kinesin motility. Bacterial expression of the first 340 amino acids of the *Drosophila* kinesin heavy chain (which contains the core NH_2-terminal globular motor domain and the first ~10 amino acids of the neck) produces a monomeric protein that generates directed motility when many motors are interacting simultaneously with a single microtubule in gliding motility assays (7, 13). However, these monomeric kinesins do not exhibit processive movement when assayed as individual motors in a single molecule fluo-

* This research was supported by the Medical Research Council of Canada and a studentship (to B. T.) from the Alberta Heritage Foundation for Medical Research, Alberta, Canada. The costs of publication of this article were defrayed in part by the payment of page charges. This article must therefore be hereby marked "*advertisement*" in accordance with 18 U.S.C. Section 1734 solely to indicate this fact.

‖ To whom correspondence should be addressed: Dept. of Biochemistry, University of Alberta, Edmonton, Alberta T6G 2H7, Canada. Tel.: 403-492-2758; Fax: 403-492-0095.

rescence motility assay (14) or a bead assay (15). A kinesin motor containing the complete motor and neck domains, on the other hand, forms a dimer and also exhibits processive movement (14, 16). Collectively, these studies suggest that the dimeric structure of kinesin is not essential for force-generation *per se*, although it does appear to be required for processive movement. This raises the possibility that processive movement may involve a hand-over-hand coordination of the two kinesin heads.

The proposed α-helical coiled-coil domain in the kinesin neck may be structurally important for coordinating the activities of the two kinesin heads during processive movement. The existence of a coiled-coil structure in close proximity to the motor domains, however, raises important questions concerning its exact boundaries and stability, since the connection between the heads must be sufficiently extensible to allow the two motor domains to span the distance between two tubulin dimers during movement. It is also important to determine the thermodynamic properties of the neck coiled-coil to ascertain if it could partially or totally "un-coil" during the generation of a power stroke. Unfortunately, the atomic resolution structure of the neck domain is unknown, since the segment between residues 323 and 349 is disordered and hence invisible in the present electron density maps of human kinesin (hK349) (2). Thus, to gain insight into the structure of the kinesin neck region and its possible functional roles, we have investigated the secondary structure of the human kinesin heavy chain neck region using several synthetic peptides in conjunction with CD spectroscopy.

In the present study, we report that a two-stranded, α-helical coiled-coil dimerization domain exists between residues 330–369 within the human kinesin neck region, as predicted from previous work. Residues located to the COOH terminus of this region, 370–383, appear to be unstructured and are not significantly involved in further stabilization of the dimerization domain. Residues located to the NH_2 terminus of the proposed coiled-coil dimerization domain may adopt a β-sheet secondary structure. Analysis of the stability of each peptide indicates that the heptads required to form a stable coiled-coil domain are arranged in a strong-weak-strong manner. Loss of two heptads from either the NH_2 or COOH terminus significantly affects dimer stability. These results suggest that a conformational change in the motor domain, driven by a free energy change associated with ATP hydrolysis, could be transmitted in a manner that affects the stability and/or conformation of the adjacent neck region. We propose a model for kinesin motility in which unwinding of a portion of the coiled-coil domain plays an important role in the mechanochemical cycle.

MATERIALS AND METHODS

Peptide Synthesis and Purification—Synthetic kinesin peptides were prepared by solid-phase synthesis methodology using a 4-benzylhydrylamine hydrochloride resin with conventional *N-t*-butyloxycarbonyl chemistry on an Applied Biosystems model 430A peptide synthesizer as described by Sereda *et al.* (17). Peptides were cleaved from the resin by reaction with hydrogen fluoride (20 ml/g resin) containing 10% anisole and 2% 1,2-ethanedithiol for 1 h at −5 °C, washed with cold ether several times, extracted from the resin with glacial acetic acid, and then lyophilized. Purification of each peptide was performed by reversed-phase high performance liquid chromatography (RP-HPLC)[1] on a SynChropak semi-preparative C-8 column (250 × 10 mm, inner diameter, 6.5-μm particle size, 300-Å pore size; SynChrom, Lafayette, IN) with a linear AB gradient (ranging from 0.2 to 1.0% B/min) at a flow rate of 2 ml/min, where solvent A is aqueous 0.05% trifluoroacetic acid and solvent B is 0.05% trifluoroacetic acid in acetonitrile. Homogeneity of the purified peptides were verified by analytical RP-HPLC, amino acid analysis, and electrospray quadrapole mass spectrometry.

Preparation of Oxidized Peptides—Oxidation of kinesin peptides (formation of a disulfide bond to form a homo-two-stranded molecule) was carried out by dissolving 5 mg of peptide into 2 ml of 100 mM NH_4HCO_3, pH 8 buffer and stirring overnight in an open reaction vessel. The oxidized peptides were then re-purified by RP-HPLC and characterized by mass spectrometry (as described above).

Circular Dichroism Spectroscopy—Circular dichroism (CD) spectra were recorded on a Jasco J-720 spectropolarimeter (Jasco Inc., Easton, MD) interfaced to an Epson Equity 386/25 computer running the Jasco DP-500/PS2 system software (version 1.33a). The temperature-controlled cuvette holder was maintained at 20 °C with a Lauda model RMS circulating water bath (Lauda, Westbury, NY). The instrument was calibrated with an aqueous solution of re-crystallized *d*-10-(+)-camphorsulfonic acid at 290.5 nm. Results are expressed as mean residue molar ellipticity [Θ] (deg·cm^2·dmol^{-1}) calculated from Equation 1.

$$[\theta] = (\theta_{obs} - MRW)/(10 \times l \times c) \quad \text{(Eq. 1)}$$

Θ_{obs} is the observed ellipticity expressed in millidegrees, MRW is the mean residue molecular weight (molecular weight of the peptide divided by the number of amino acids), l is the optical path length in cm, and c is the final peptide concentration in mg/ml. For wave scans, data was collected from 190 to 255 nm at 0.05-nm intervals, and the average of 10 scans reported. Concentration dependence studies were carried out by monitoring the change in helical content at 222 nm at various peptide concentrations. GdnHCl denaturation studies were carried out by preparing mixtures of a stock solution of peptide in buffer (0.1 M KCl, 0.05 M PO_4, 0.002 M DTT, pH 7), buffer alone and a solution of 8 M GdnHCl in buffer where the ratios of buffer and 8 M GdnHCl solutions were varied to give the appropriate final GdnHCl concentrations. All peptide concentrations were determined by amino acid analysis on a Beckman model 630 amino acid analyzer.

Protein Unfolding Measurements—Denaturation midpoints, slopes, and free energy of unfolding values for the various kinesin peptides (see Table I) were determined by following the change in molar ellipticity at 222 nm using a Jasco J-720 spectropolarimeter (as described above). Ellipticity readings were normalized to the fraction of the peptide folded (f_f) or unfolded (f_u) using the standard equations shown (Equations 2 and 3).

$$f_f = ([\theta] - [\theta]_u)/([\theta]_n - [\theta]_u) \quad \text{(Eq. 2)}$$

$$f_u = (1 - f_f) \quad \text{(Eq. 3)}$$

$[\theta]_n$ and $[\theta]_u$ represent the ellipticity values for the fully folded and fully unfolded species, respectively. $[\theta]$ is the observed ellipticity at 222 nm at any denaturant concentration. The calculation of the ΔG_u^{H2O} (the free energy of unfolding in the absence of guanidine hydrochloride) was estimated by extrapolating the free energy of unfolding at each denaturant concentration to zero concentration assuming they are linearly related by the equation $\Delta G_u = \Delta G^{H2O} - m[\text{GdnHCl}]$ (18, 19). ΔG_u for reduced peptides was calculated from Equation 4 (20), where P_t is the total peptide concentration (M).

$$\Delta G_u = -RT \ln(2P_t(f_u^2/(1 - f_u)) \quad \text{(Eq. 4)}$$

Size-exclusion Chromatography with Laser Light Scattering—Molecular weights of the peptides in aqueous solution were determined by size-exclusion chromatography (SEC) with laser light scattering. SEC was carried out on a Superose 12 column (1.0 cm × 30.0 cm) from Pharmacia at a flow rate of 0.5 ml/min at room temperature. The eluent was a 100 mM KCl, 50 mM K_2HPO_4, pH 7, buffer. The effluent from the column was monitored using either a Hewlett Packard UV-visible spectrophotometer at 210 nm, or a Dawn F multiangle laser light scattering photometer connected in series with a Optilab 903 refractometer. Determination of molecular weights (by laser light scattering) was carried out according to the methodology described by Farrow *et al.* (21).

Helical Propensity/Hydrophobicity Analysis—The score for α-helical propensity and hydrophobicity (occurring in a 3–4 repeating pattern) was calculated for residues 280–420 of the kinesin protein. Each α-helical propensity data point was obtained by an iterative process involving the summing of 11 individual α-helical propensity scores (22) for the sequence starting at residue position 280. Subsequent data points were then obtained by shifting 1 residue toward the COOH terminus and repeating the process. Hydrophobicity values, occurring in a 3–4 re-

[1] The abbreviations used are: RP-HPLC, reversed-phase high performance liquid chromatography; SEC, size-exclusion chromatography; GdnHCl, guanidine hydrochloride; TFE, trifluoroethanol; DTT, dithiothreitol.

```
                          316          330          344          355          369          383
                           |            |            |            |            |            |
Kinesin                LLFGQRAKTIKNTVCVNVELTAEQWKKKYEKEKEKNKILRNTIQWLENELNRWRNGETVPIDEQFDKE

K1 (316-355)        Ac-LLFGQRAKTIKNTVCVNVELTAEQWKKKYEKEKEKNKILR-amide

K2 (330-369)                     Ac-CVNVELTAEQWKKKYEKEKEKNKILRNTIQWLENELNRWR-amide

K3 (344-383)                                 Ac-YEKEKEKNKILRNTIQWLENELNRWRNGETVPIDEQFDKE-amide

K4 (316-369)        Ac-LLFGQRAKTIKNTVCVNVELTAEQWKKKYEKEKEKNKILRNTIQWLENELNRWR-amide

K5 (330-383)                     Ac-CVNVELTAEQWKKKYEKEKEKNKILRNTIQWLENELNRWRNGETVPIDEQFDKE-amide


Kinesin Analogs

K6                                           Ac-[EIEALKAEIEALKAEIEALKAEIEALKA]GETVPIDEQFDKE-amide
                                                *  *  *
K7                                           Ac-[EYEAEKAENEALKAEIEALKAEIEALKA]GETVPIDEQFDKE-amide
                                                *  *  *
K8                                           Ac-KIEKLKEKIKILRNTIQWLENELNRWRNGETVPIDEQFDKE-amide
```

FIG. 1. **Amino acid sequences of the kinesin peptides used in this study.** The native human kinesin sequence is shown at the *top*. Residues proposed to be involved in forming the 3–4 hydrophobic repeat of a coiled-coil are *underlined*. Peptide names are indicated on the *left*. *Numbers* in *parentheses* indicate the region of the amino acid sequence which the peptide spans. *Ac-* denotes N^{α}-acetyl, and -amide denotes C^{α}-amide. The three kinesin analogs are shown below. Residues of the native kinesin sequence which have been replaced by a model coiled-coil sequence are *boxed*. The location of amino acid substitutions in either the native or model coiled-coil sequences are indicated by an *asterisk* (*). The position of all kinesin peptides and analogs are shown relative to the native sequence.

peating pattern, were calculated in a similar manner by summing the hydrophobicity scores (22) for the first 6 residues that occur in a "3–4" repeating pattern (*i.e.* residues 1, 4 8, 11, 15, and 18). Subsequent data points for the same face were then calculated by shifting first 3 residues (4, 8, 11, 15, 18, and 22), then 4 residues (8, 11, 15, 18, 22, and 25), and so forth throughout the sequence to maintain the same reading frame. Calculation of the other six faces was carried out by starting +1 residue toward the COOH terminus (2, 5, 9, 12, 16, and 19) etc. to obtain data for the second face and another +1 residue shift (3, 6, 10, 13, 17, and 20), etc., for face 3. This process is repeated to obtain data for faces 4 to 7.

RESULTS

CD Analysis of the Kinesin Neck Peptides—To examine the structural characteristics of the human kinesin neck region, several synthetic peptides (see Fig. 1 for sequences) that span various regions between residues 316 and 383 were prepared and analyzed by circular dichroism (CD) spectroscopy. Fig. 2 (*panels A* and *B*) shows the far UV CD spectra for the kinesin peptides K1–K5. Kinesin peptides K2, K3, K4, and K5 all show characteristic α-helical spectra with double minima at 208 and 222 nm (23, 24). The K2 peptide, which represents residues 330–369 of the kinesin neck region, displayed the greatest molar ellipticity (−24,600°), corresponding to ~70% α-helical content or ~28 helical residues (see Table I). The addition of two heptads (14 residues) onto the COOH terminus of this region (K5, 330–383) results in a decrease in the molar ellipticity to −19,500°, indicating that the COOH-terminal residues 370–383 added are not α-helical. The calculation of the helical content for K5 is 54% or ~29 helical residues, which indicates no loss of the existing helical residues from the region 330–369. The addition of two heptads onto the NH_2 terminus of this region (K4, 316–369) also results in a significant decrease in the molar ellipticity to −13,300°, again indicating the addition of non-helical residues onto the helical domain located between 330 and 369. Calculation of the helical content for the peptide K4 is 37% or ~20 helical residues, which represents a loss of ~8 helical residues from the region 330–369. Analysis of the kinesin peptide K3 (344–383), which represents a 40-residue peptide shifted two heptads (14 residues) toward the COOH terminus, shows a molar ellipticity at 222 nm of −16,500°, corresponding to a helical content of 46% or ~19 helical residues. This represents a loss of ~9 helical residues for the deletion of the two heptads 330–343, indicating that the two

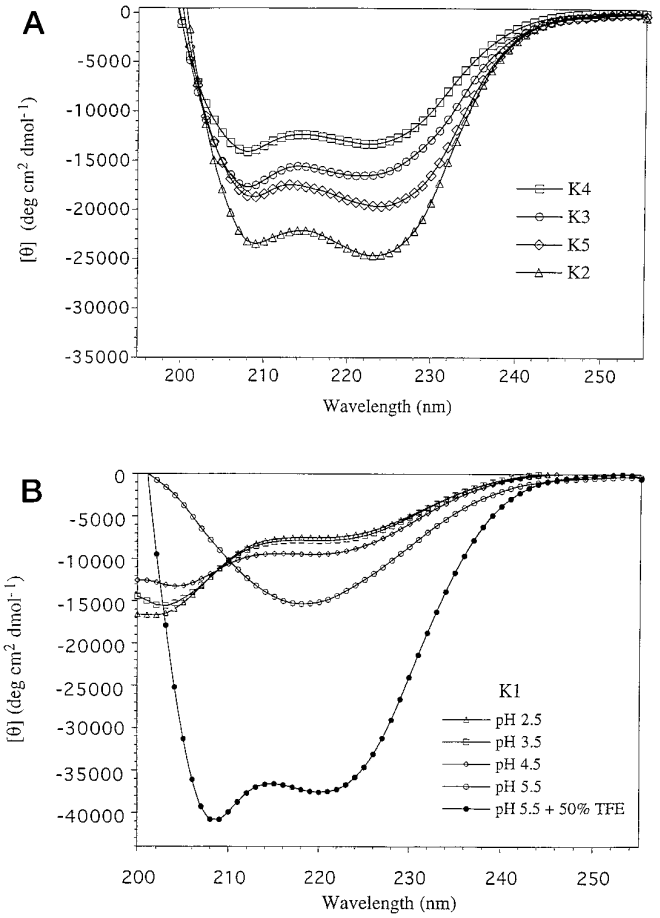

FIG. 2. **CD spectra of the kinesin peptides.** *Panel A*, CD spectra for kinesin peptides K2–K5; spectra were recorded at 20 °C in a 0.1 M KCl, 0.05 M PO_4, 0.002 M DTT, pH 7 buffer. All peptide concentrations were 100 μM. *Panel B*, the CD spectra of kinesin peptide K1 at various pH levels and in the presence of 50% TFE. Spectra were recorded at 20 °C in a 0.1 M KCl, 0.05 M PO_4, 0.002 M DTT buffer at the indicated pH. Peptide concentrations were 350 μM.

NH_2-terminal heptads of 330–343 are very important for the helical content observed in the region 330–369. One can also see from the spectra of the kinesin peptides in Fig. 2*A* that the

TABLE I
Ellipticities and stabilities of the synthetic kinesin peptides

Peptide[a]	$[\theta]_{222}$[b]		Helical content[c]		$[GdnHCl]_{1/2}$[d]	$\Delta G_u^{H_2O}$[e]	m[f]	$\Delta\Delta G_u$[g]
	Benign	50% TFE	%	No. of residues				
	degrees · cm² · dmol⁻¹				M	*kcal · mol⁻¹*		
K2	−24,600	−26,600	70	28	3.61	10.42	1.205	0.0
K2 oxid.	−26,600	−32,200	74	30	5.22			
K3	−16,500	−19,190	46	19	1.17	8.46	2.285	1.96
K4	−13,300	−18,440	37	20	3.73	10.14	1.125	0.283
K5	−19,500	−21,200	54	29	3.93	10.31	1.143	0.105
K5 oxid.	−23,200	−27,900	64	34	5.54			
K6	−25,000	−25,560	70	29	>7.0	>20		
K7	−22,200	−25,380	62	25	2.73	10.18	1.208	
K8	−18,700	−20,500	52	21	3.58	11.20	1.195	2.74[h]

[a] The amino acid sequences for each peptide are shown in Fig. 1.
[b] The mean residue molar ellipticities at 222 nm were measured at 20 °C in benign buffer (0.1 M KCl, 0.05 M PO_4, pH 7). For samples containing TFE, the above buffer was diluted 1:1 (v/v) with TFE. Peptide concentrations were 100 μM.
[c] The (%) helical content was calculated from the ratio of the observed $[\theta]_{222}$ value divided by the predicted molar ellipticity × 100. The predicted molar ellipticity was calculated from the equation $[\theta]_{222} = 40 \times 10^3 \times (1–4.6/n)$ for the chain length dependence of an α-helix (24, 58), where n is the number of residues in the peptide. The number of helical residues was calculated by multiplying the % of helical content × the total number of residues in the peptide.
[d] $[GdnHCl]_{1/2}$ is the transition midpoint, the concentration of guanidine hydrochloride (M) required to give a 50% decrease in the molar ellipticity at 222 nm.
[e] $\Delta G_u^{H_2O}$ is the free energy of unfolding in the absence of guanidine hydrochloride and was estimated by extrapolating the free energy of unfolding at each denaturant concentration to zero concentration assuming the linear relationship $\Delta G_u = \Delta G^{H_2O} - m[GdnHCl]$ (18, 19). ΔG_u was calculated from the equation $\Delta G_u = -RT \ln (2P_t (f_u^2/(1 - f_u))$ for reduced peptides. f_u is the molar fraction of denatured peptide as determined from the ellipticity at 222 nm and P_t is the total peptide concentration (M).
[f] m is the slope in the equation $\Delta G_u = \Delta G_u^{H_2O} - m[GdnHCl]$.
[g] The difference in the free energy of unfolding ($\Delta G_u^{H_2O}$) relative peptide K2.
[h] Indicates the stability difference relative to peptide K3.

ratios of $[\theta]_{222}$ to $[\theta]_{208}$, which are often used as an indication of coiled-coil formation, are >1 for K2 and K5, but <1 for K3 and K4, suggesting a transition from a possible two-stranded α-helical coiled-coil to a single-stranded α-helix (25–30).

CD analysis of the kinesin peptide K1 (residues 316–355), which represents a 40-residue peptide shifted two heptads toward the NH_2 terminus (from the region 330–369), reveals a complete absence of α-helical content. In fact the secondary structure of this peptide now displays a β-sheet pattern (23). It is important to note, however, that the spectrum of this peptide could not be acquired under the same benign conditions like those used for the other peptides. At pH 2.5, K1 is highly soluble and shows only a random coil spectrum. Increasing the pH successively from 2.5 to 5.5 results in a major transition from a largely random coil spectrum to that of a β-sheet spectrum, with the greatest transition occurring between pH 4.5 and 5.5. Analysis of the peptide above pH 5.5 was not possible due to the complete gelation of the solution. The pH dependence of this transition (pH 4.5–5.5) suggests that the ionization of glutamic acid residues are involved. Unfortunately, it is not possible to ascertain from these results whether formation of the β-sheet secondary structure is a result of intramolecular or intermolecular interactions, or a combination of both. However, our observations with K4 (which contains this region) showing a loss in helical content of ~8 residues but no substantial loss in stability compared with K2 (discussed below) suggests that their is some intramolecular formation at the NH_2 terminus of this peptide. The gelation of the solution also suggests the formation of intermolecular association as well.

Interestingly, in the presence of 50% TFE, a helix-inducing solvent (26, 31), the K1 peptide reverts to a fully α-helical spectrum (equal to that calculated for a 40-residue peptide (23, 24). This result indicates that this region of kinesin has the intrinsic ability to adopt either β-sheet or helical secondary structures depending on the environment. It should be noted that the first few amino acids of this peptide (316–320) are in a helical configuration in the kinesin crystal structure (2).

Oxidation of Cys^{330}—Although the α-helical content of the K2 peptide (residues 330–369) is significantly greater than that of the other native kinesin peptides, it still does not represent a fully helical structure as calculated theoretically for a 40-residue peptide (~−36,500°) (24). We therefore determined if oxidation of the NH_2-terminal cysteine (Cys^{330}) to form a disulfide bridge could increase the helical content to that of the theoretical value by stabilizing the ends of the proposed coiled-coil as well as by making the coiled-coil dimerization domain concentration independent (29, 32, 33). When the peptide was oxidized, a change in its molar ellipticity was observed (see Fig. 3). Oxidation only slightly increased the molar ellipticity at 222 nm by approximately 2000°, which is similar to that obtained for the reduced K2 peptide in the presence of 50% TFE, a helix-inducing solvent (26, 31). This degree of ellipticity indicates that the reduced (monomeric) K2 peptide is almost fully helical (93%) if judged by the maximal amount of helical content that can be induced either in an oxidized state or in 50% TFE. Although previous studies have shown that theoretical maximum values are not always observed for helical peptides, the observation of a lower molar ellipticity than the theoretical value may also be indicating that there is a region within residues 330–369 that cannot be induced into a fully α-helical structure by either a helix-inducing solvent or oxidation. The central region containing residues Tyr^{344}, Glu^{347}, and Asn^{351} in the hydrophobic core is a good candidate for such a region and will be discussed further below.

Two further points can be made regarding the oxidation results. First, the finding that the α-helical secondary structure for the K2 peptide is enhanced instead of disrupted by disulfide bond formation indicates that the two peptides interact in a parallel and in-register manner. Second, while disulfide bond formation of Cys^{330} can occur in a peptide, this may not be possible when the neck is joined to the globular motor domain. This cysteine is also not conserved among conventional kinesin motor proteins from different species.

Stability and Concentration Dependence of the Kinesin Peptides—An important question raised regarding the existence of a coiled-coil within the neck region was whether it alone is sufficiently stable to account for the dimerization of the kinesin

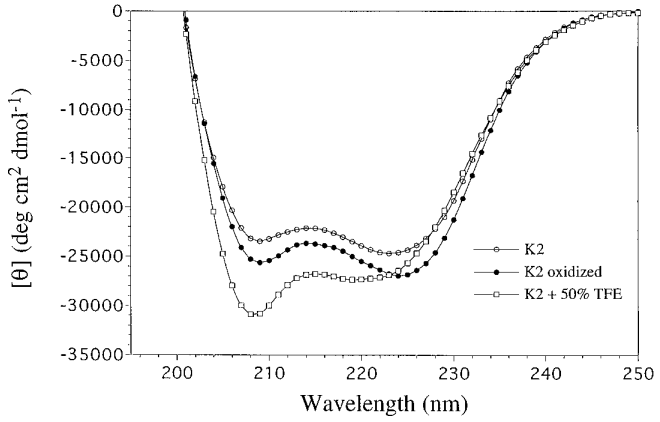

FIG. 3. **CD spectra of the K2 peptide in the reduced and oxidized state, as well as in the presence of 50% TFE.** Spectra were recorded in a 0.1 M KCl, 0.05 M PO_4, pH 7 buffer. 2 mM DTT was present for the reduced and 50% TFE scans. Peptide concentrations were 100 μM.

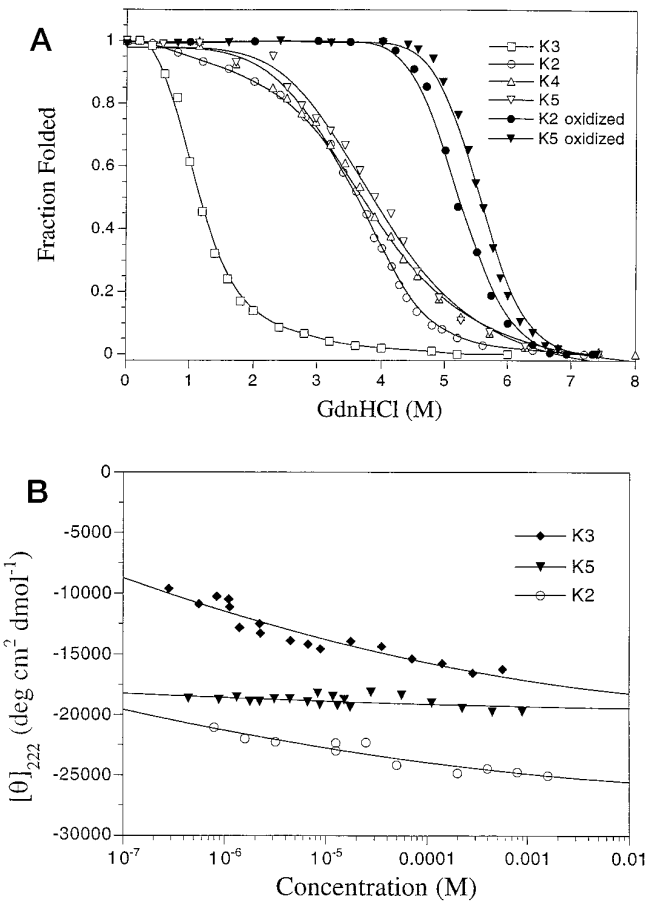

FIG. 4. *Panel A*, denaturation profiles of kinesin peptides K2–K5 at 20 °C in 0.1 M KCl, 0.05 M PO_4, 0.002 M DTT (omitted when oxidized), pH 7 buffer with GdnHCl denaturant. The fraction folded (f_f) of each peptide was calculated as $f_f = ([\theta] - [\theta]_u)/([\theta]_n - [\theta]_u)$, where $[\theta]$ is the observed mean residue ellipticity at 222 nm at any particular denaturant concentration and $[\theta]_n$ and $[\theta]_u$ are the mean residue ellipticities at 222 nm of the native "folded" and "unfolded" states, respectively. Each peptide was analyzed at a 60 μM concentration. *Panel B*, concentration dependence of the mean residue molar ellipticity at 222 nm for kinesin peptides K2, K3, and K5. Ellipticities were recorded in the same buffer as described above, using various pathlength cells (0.05, 0.1, and 1 cm) depending on the peptide concentration.

motor domain heads or whether other subunit-subunit interactions are also involved. To address this question, we determined the stability of the five kinesin peptides by GdnHCl denaturation (Fig. 4*A*). The K2 peptide (330–369), which showed the greatest α-helical content (Fig. 2), displayed a GdnHCl midpoint of 3.61 and an extrapolated ΔG_u^{H2O} of unfolding of 10.42 kcal/mol, indicating a very stable α-helical structure. The K4 peptide (316–369), which showed a decrease in the helical content and calculated α-helical residues, showed a similar GdnHCl midpoint and ΔG_u^{H2O} of unfolding (compare K2 and K4, Table I). Thus the apparent loss of helical residues at the NH_2 terminus of the coiled-coil region is apparently compensated by the formation of an alternative structure or interaction of similar stability.

The K5 peptide (330–383), the COOH-terminal residues (370–383) of which are non-helical, also showed a similar GdnHCl midpoint and ΔG_u^{H2O} of unfolding (compare K2 and K5, Fig. 3*A*, and Table I), indicating that the COOH-terminal residues do not significantly affect the stability of the α-helical structure. The small difference that is observed in the GdnHCl midpoints may be due to end effect stabilization (32). The stability of the K3 peptide (344–383), which showed a decrease in the helical content and loss of helical residues, was significantly destabilized (GdnHCl midpoint of 1.17) by the loss of the two NH_2-terminal heptads (330–343), indicating that these two heptads are very important in the stability of the proposed α-helical coiled-coil structure. Oxidation of both the K2 and K5 peptides resulted in significant increases in their GdnHCl midpoints (from 3.61 to 5.22 and 3.93 to 5.54, respectively), which indicates that the formation of a disulfide bonds stabilizes the α-helical structure as seen in other studies (29, 32, 33).

The concentration dependence of the α-helical content, which can also be used as an indicator of the stability of the associated coiled-coils, was determined for kinesin peptides K2, K3, and K5. Fig. 4*B* shows that the helical content for K2 and K5 is largely unaffected by concentration over the range tested, indicating that they are very tightly associated α-helical structures. The equilibrium association constants from the GdnHCl denaturation plots for K5 and K2 are estimated to be 2.7×10^8 M^{-1} and 2.3×10^8 M^{-1}, respectively. The similar values for K2 and K5 indicate that the the stability and association of the structure resides principally within residues 330–369. The effect of deleting the two NH_2-terminal heptads (residues 330–343) from K5 (giving peptide K3) shows a greater dependence of the α-helical content with peptide concentration. Quite surprisingly, however, the difference in the concentration dependence of K3 and K2 was not as dramatic as expected from the difference in their stability (Fig. 4*A*). This result may indicate that electrostatic interactions also play a significant role in the association between the two α-helices in K3 (predominantly electrostatic interactions are quickly quenched by GdnHCl denaturation and thus not seen as a major stabilizing factor).

Size-exclusion Chromatography with Laser Light Scattering—To determine the oligomerization state of the α-helical structures in an aqueous solution, size-exclusion chromatography with laser light scattering detection was conducted. Representative SEC chromatograms for the K5 and K3 peptides are shown in Fig. 5. Analysis of kinesin peptide K5 in the oxidized and reduced states showed only a single eluting peak with an apparent molecular weight obtained from light scattering of 11,702 Da. This value is close to that predicted for a dimeric structure (13,460 Da). The observation of only a single species indicates that K5 peptide forms a very stable, dimeric structure, which agrees with the data presented previously. Similar studies conducted with K2 (data not shown) also produced only one peak corresponding to a dimeric molecular weight. On the other hand, the K3 peptide eluted in two peaks: the first dominant peak having an apparent molecular mass of

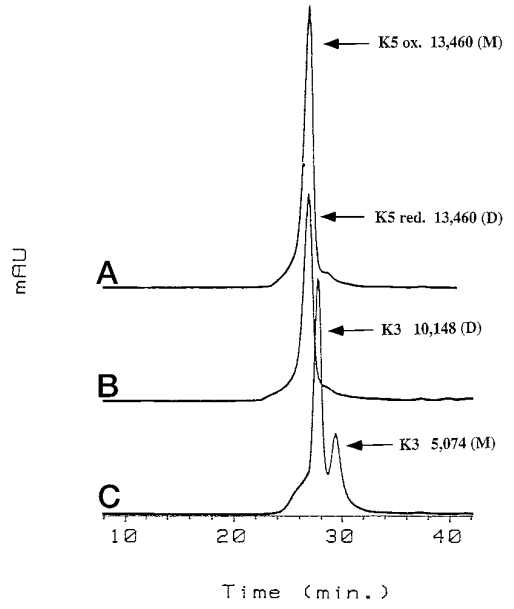

FIG. 5. **SEC of the kinesin peptides.** *Run A*, K5, oxidized; *run B*, K5, reduced; *run C*, K3. The column used was Superose 12 (1.0 cm x 30.0 cm) from Pharmacia. Running conditions were as follows: mobile phase, 100 mM KCl, 50 mM K_2HPO_4, pH 7 buffer; flow rate, 0.5 ml/min; temperature, 26 °C; detection, 210 nm using a Hewlett Packard UV-visible spectrophotometer. Molecular weights for each peptide are indicated as well as the observed oligomerization state: *(M)* denotes monomer; *(D)* denotes dimer.

9,285 Da and the second smaller peak having a molecular weight (5,854 Da) close to that of the monomeric peptide (5,074 Da). The observation of dimer and monomer peaks is consistent with previous data showing that the K3 peptide exhibits the greatest concentration dependence for helical content. Thus, SEC, CD spectroscopy, and stability studies all suggest that a stable, two-stranded α-helical coiled-coil can form between two chains of the kinesin neck region and that residues 330–369 are the ones of primary importance for the formation of this structure.

Destabilizing Effects of Tyr^{344}, Glu^{347}, and Asn^{351} in the Hydrophobic Core—Previous studies have shown that the stability of two-stranded α-helical coiled-coils is dependent upon the helical propensity of the region, hydrophobicity of the residues in the core, packing of residues in the core, electrostatic interactions adjacent to the core, and chain length effects (27–29, 34–40). In the kinesin neck region, several of the residues that are predicted to exist within the hydrophobic core are considered to be "non-ideal" for generating a stable coiled-coil. Particularly noticeable are residues Tyr^{344}, Glu^{347}, and Asn^{351} that score relatively low by hydrophobicity analysis and thus are not expected to contribute significantly to stability. In particular, the ionized carboxyl group of glutamic acid has been shown to be extremely destabilizing in model coiled-coils.[2] To examine the effects of residues Tyr^{344}, Glu^{347}, and Asn^{351} on coiled-coil stability, we prepared and analyzed three analog peptides (see Fig. 1 for sequences). First, we prepared a kinesin peptide analog (K6) in which the four heptads of the native kinesin sequence between residues 344–370 were replaced by a model coiled-coil sequence that has been previously characterized (39). Second, in the K7 analog, the three "destabilizing" kinesin hydrophobic core residues, Tyr^{344}, Glu^{347}, and Asn^{351}, were substituted into the above model coiled-coil sequence. Finally, in K8, three high stability hydrophobic core residues from the "model" coiled-coil (leucine and isoleucine) were substituted into the native kinesin sequence into positions 344, 347, and 351.

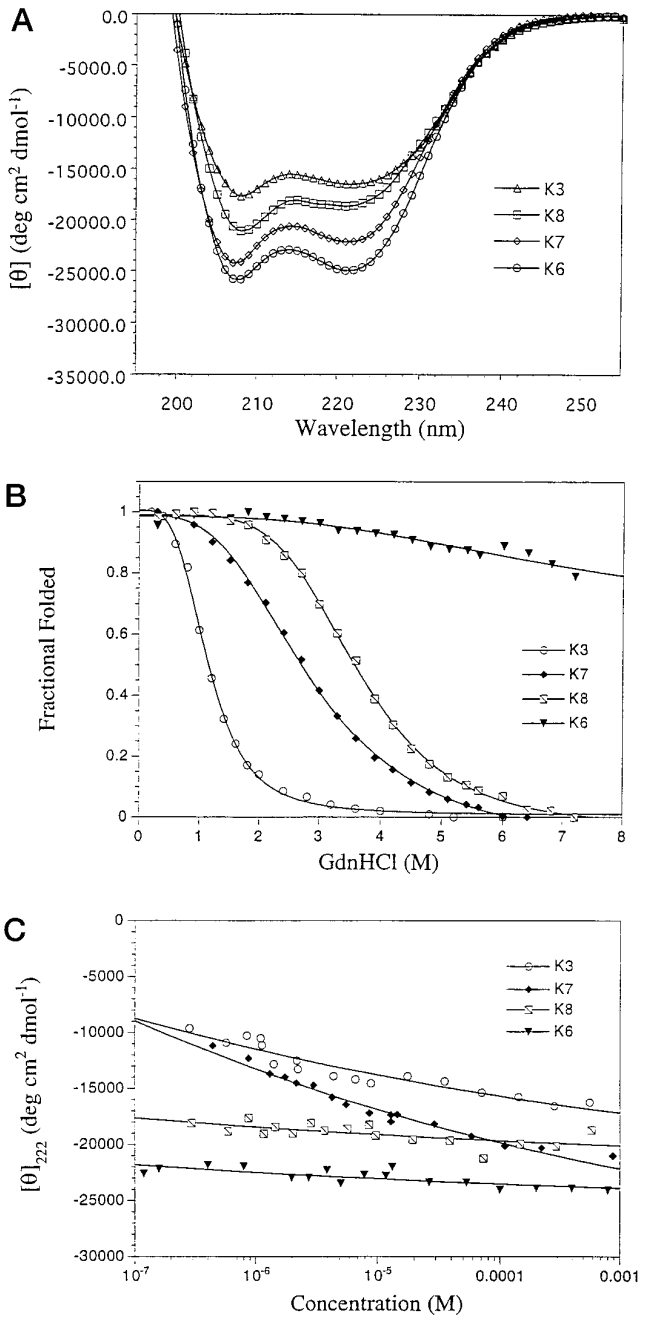

FIG. 6. **Effects of substituting Tyr^{344}, Glu^{347}, and Asn^{351}.** *Panel A*, CD spectra for the kinesin analogs K6, K7, and K8 were recorded at 20 °C in 0.1 M KCl, 0.05 M PO_4, 0.002 M DTT, pH 7 buffer. Peptide concentrations were 100 μM. *Panel B*, GdnHCl denaturation profiles of K6, K7, and K8 were recorded at 222 nm at 20 °C in 0.1 M KCl, 0.05 M PO_4, 0.002 M DTT, pH 7 buffer. The fraction folded (f_f) was calculated as described in Fig. 4. Peptide concentrations were 60 μM. *Panel C*, concentration dependence of the mean residue molar ellipticity at 222 nm were measured at 20 °C in 0.1 M KCl, 0.05 M PO_4, 0.002 M DTT, pH 7 buffer as described in Fig. 4. For direct comparison of the three analogs to that of the native sequence, K3 (previously shown in Figs. 2 and 4) is shown again in all three plots.

Fig. 6*A* shows the secondary structure content of the three kinesin analogs relative to the unsubstituted kinesin peptide K3 (344–383). All three of the kinesin analogs show characteristic double minimas at 208 and 222 nm typical for α-helical protein structures (23, 24). As expected, K6 (the model coiled-coil sequence) displayed the greatest molar ellipticity (39). In-

[2] B. Tripet, R. D. Vale, and R. S. Hodges, unpublished results.

troduction of the three kinesin hydrophobic core residues Tyr^{344}, Glu^{347}, and Asn^{351} into the K6 sequence caused a significant decrease in the molar ellipticity (compare K6 and K7, Fig. 6*A*), suggesting a disruption between the two associated α-helices as well as a decrease in coiled-coil stability. Conversely, replacement of Tyr^{344}, Glu^{347}, and Asn^{351} with the "ideal" hydrophobes from the model sequence in K8 resulted in an increase in molar ellipticity, suggesting an increase in coiled-coil stability and association compared with the native kinesin sequence (K8 *versus* K3 in Fig. 6*A*).

To verify that the changes in helical content observed are in fact a result of changes in the stability of the respective coiled-coils, we determined the stability of K6, K7 and K8 by GdnHCl denaturation (Fig. 6*B* and Table I). The introduction of kinesin Tyr^{344}, Glu^{347}, and Asn^{351} into the model coiled-coil sequence caused a dramatic decrease in the stability (compare K6 and K7, GdnHCl midpoints of >8 and 2.73, respectively). Correspondingly, the introduction of the three ideal model hydrophobic residues into the kinesin sequence dramatically increased the stability of the kinesin peptide K3 by 2.74 kcal/mol (GdnHCl midpoints of 1.17 and 3.58 for K3 and K8, respectively).

The changes in stability observed in Fig. 6*B* are also reflected in the concentration dependence of the helical content, as measured at 222 nm (Fig. 6*C*). The model coiled-coil sequence K6 exhibited practically no concentration dependence, which is consistent with its high degree of stability. Introduction of kinesin residues Tyr^{344}, Glu^{347}, and Asn^{351} into this sequence caused the coiled-coil now to dissociate upon dilution (compare K6 and K7, Fig. 6*C*). Conversely, introduction of the ideal hydrophobes into the native kinesin sequence (K8) dramatically decreased its concentration dependence, which is consistent with its increased stability (compare K3 and K8, Fig. 6*B*). Collectively, these data indicate that residues Tyr^{344}, Glu^{347}, and Asn^{351} destabilize the central region of the coiled-coil domain in kinesin. It is intriguing that both positions Tyr^{344} (Tyr or Phe) and Glu^{347} are very well conserved in the neck domains of the conventional kinesin, bimC/Eg5, and Kif3 (heterotrimeric) subfamilies of kinesin motors.[3]

Predictions of Helical Propensity and Hydrophobicity in the Kinesin Neck—Finally, we wished to determine whether the observed location of the coiled-coil dimerization domain (residues 330–369) agrees with a predictive method developed in our own laboratory. The criteria of our method for predicting coiled-coil regions, which is very similar to that used by others, is based on the fact that coiled-coil regions are typically high in α-helical propensity (which exists over a minimum of 21 successive residues) as well as amphipathic, with hydrophobic residues occurring in a 3–4 repeating pattern. Analysis of the helical propensity of human kinesin sequence between residues 280 and 420 shows that there are three regions of high helical propensity that are well above our statistically determined cut-off value of 440.[2] These regions are indicated by the *three connected boxes* shown above the plot in Fig. 7*A*. Of the three helical sections, only the region spanning residues 332–369 meets the minimum 21 successive residue cut-off. This prediction agrees well with the experimentally observed stability of peptide K2 (residues 330–369). The residues adjacent to 369 dramatically drop in helical propensity, which is in agreement with our experiments showing that residues 370–383 do not add any helical content to that of the region 330–369. Residues NH_2-terminal to 332 also drop in helical propensity, which is again consistent with our results. It is interesting that the region from residue 325 to 340, which shows a large dip in

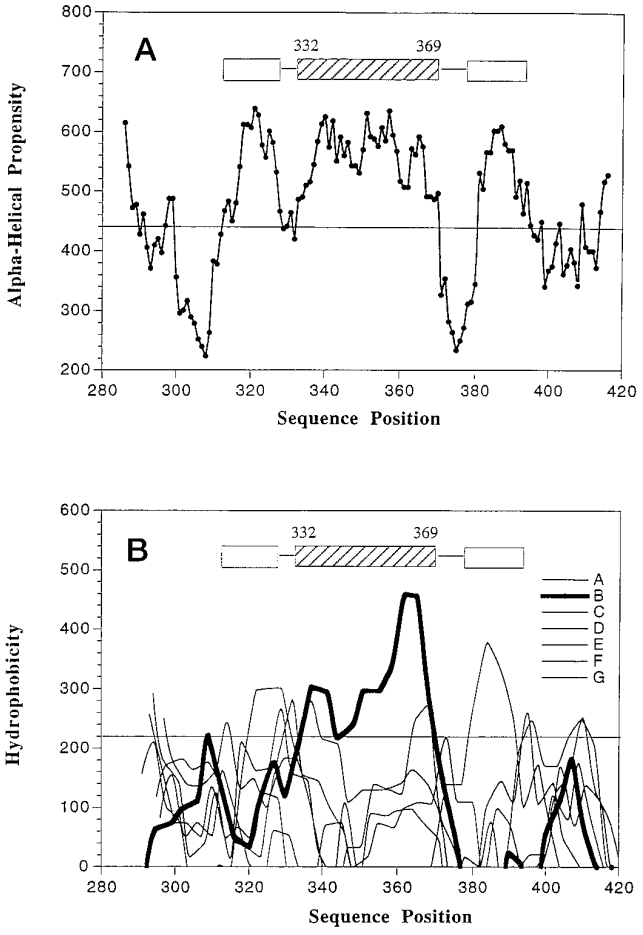

FIG. 7. **Helical propensity and hydrophobicity of the kinesin neck region.** *Top*, plot of the helical propensity from residues 280 to 420 of the human kinesin heavy chain. Each point represents the sum of 11 consecutive helical propensity scores. Regions that score greater than a pre-determined cut-off value of 440 are indicated by the *rectangular boxes*. Regions that contain >21 consecutive residues (3 heptads) above the cut-off value are indicated by *hatching*. *Bottom*, plot of the hydrophobicity occurring in a 3–4 repeating pattern of the kinesin neck region from residues 280 to 420. Each data point represent the sum of the hydrophobicity scores for six consecutive "*a*" and "*d*" positions in a coiled-coil. All seven starting faces are shown. The face with the greatest hydrophobicity occurring in the region of high helical propensity is shown in *bold*. *Face B* corresponds to residues underlined in the native kinesin sequence in Fig. 1.

helical propensity centered around residue 330, was predicted by Huang *et al.* (6) to be high in β-sheet propensity based upon the secondary structure prediction program of Holly and Karplus (41). The peptide K1 (316–355), which spans this region, appears to adopt β-sheet secondary structure at pH 5.5.

Analysis of hydrophobicity occurring in a 3–4 repeating pattern (Fig. 7B) shows that there is only one dominant hydrophobic face in the region of high helical propensity. This face (B) contains the following hydrophobic residues (see also Fig. 1) (Sequence 1).

```
330                    347                    368
-C--V---A--W---Y--E---N--L---I--L---L--W
```

SEQUENCE 1

The choice of these residues agrees with those previously predicted using the Lupus algorithm (Fig. 1, *underlined residues*) (42). The hydrophobicity of the heptad repeats appear to fluctuate dramatically. The greatest hydrophobicity occurs near the COOH terminus (hydrophobic residues of L, I, L, L, and W), an intermediate hydrophobicity is seen near the NH_2

[3] R. Case and R. Vale, manuscript in preparation.

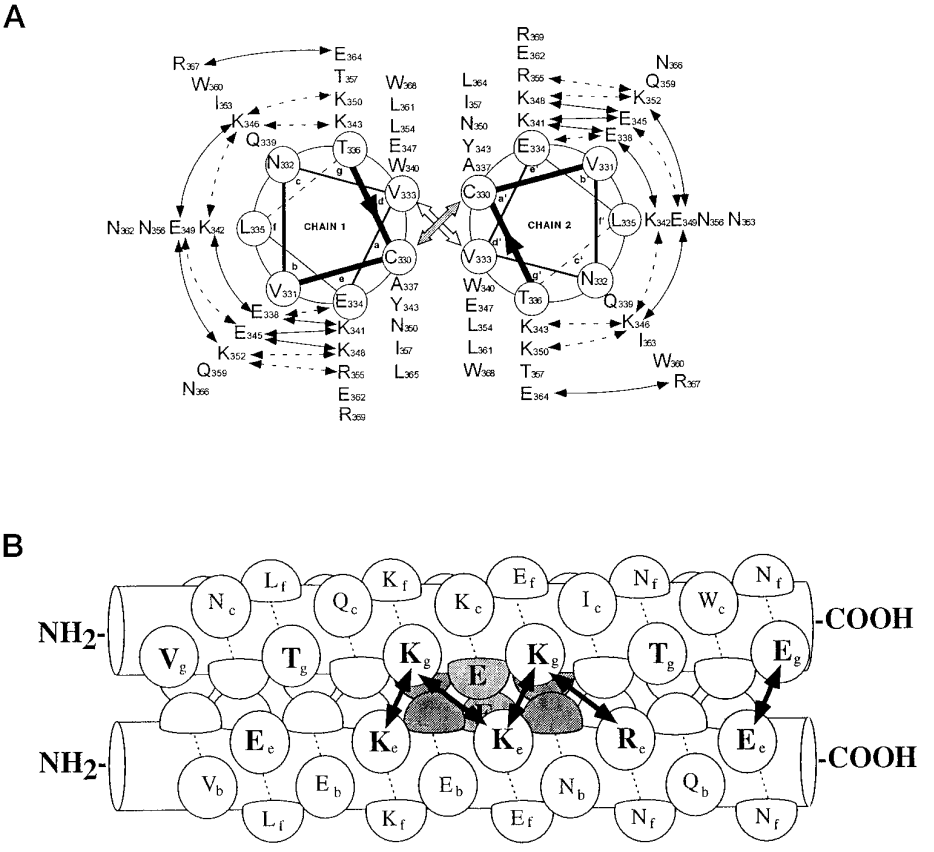

FIG. 8. **End and side views of a two-stranded α-helical coiled-coil model for residues 330 to 369 of the kinesin neck region.** *Panel A*, view from the NH_2 terminus, starting at residue 330. The direction of propagation of the peptide chains is into the page from NH_2 to COOH terminus with the chains parallel and in register. Residues in the first two helical turns are *circled*. Heptad positions are labeled *a–g*, with the *prime* indicating corresponding positions on the opposing helix. *Wide arrows* depict the hydrophobic interaction that occur between residues in the *a* and *d* positions. Possible electrostatic interactions (attractions and repulsions) occurring on the outside of the helices are indicated as *solid* and *broken* arrows respectively. *Panel B*, side view. Residues in positions *b*, *c*, *e*, *f*, and *g* are shown. Residues in the *e* and *g* positions are in *bold*. Potential electrostatic interactions occurring across the hydrophobic face are indicated. The positions for Tyr^{344}, Glu^{347}, and Asn^{351} within the hydrophobic core are *shaded*.

terminus (residues C, V, A, and W), and the weakest hydrophobic heptad repeats are centered around Y, E, and N (discussed previously). Although the results show fluctuating hydrophobicity within the proposed α-helical region, there is still significant hydrophobicity occurring in a 3–4 repeating pattern over a "large enough" range to predict that a coiled-coil could form. Thus, these results agree with those experimentally observed.

DISCUSSION

Distinct Subdomains of the Kinesin Neck—Using several synthetic peptides that overlap within the human kinesin heavy chain neck region (residues 316–383), we have been able to identify distinct subdomains with different secondary structure using CD spectroscopy. The central region from residue 330 to 369 of human kinesin heavy chain shows all of the characteristics of a stable two-stranded α-helical coiled-coil. This region shows a significant α-helical spectrum with double minima at 222 and 208 nm, as well as a ratio of $[\theta]_{222}/[\theta]_{208}$ of 1.06, which is often indicative of such structures (29–30). Furthermore, the location of this "coiled-coil" region correlates well with our own coiled-coil prediction method based on helical propensity and hydrophobicity. Stability, concentration dependence, and gel filtration analyses have indicated that the 330–369 coiled-coil region forms a very stable and tightly associated dimer. Hence, we refer to the 330–369 region of the neck as the "dimerization domain." We have also been able to establish that the dimer is most likely oriented in a parallel fashion, since oxidation of cysteine 330 preserves the helical content and only enhances the stability. This would occur only if a disulfide bond was formed between two parallel-oriented chains. These results agree with previous reports that the kinesin heavy chains are arranged in a parallel and in-register orientation (11). Hence, this work conclusively shows that the kinesin neck contains a region that is capable of forming a two-stranded α-helical coiled-coil, as had been previously suggested by sequence predictions (6, 7).

The determined location of the dimerization domain also agrees with the results of Huang *et al.* (6) and Correia *et al.* (43), who showed that *Drosophila* kinesin heavy chains truncated to residue 392 and 401, respectively, form stable dimers (these residues are equivalent to human residues 384 and 393). In addition, similar findings with synthetic kinesin neck peptides to those described here have now also been obtained by Morii *et al.* (44).

One of the questions raised from the previous work on truncated kinesin heavy chains was whether the putative coiled-coil in the neck region was sufficient on its own to account for dimerization, or whether other interactions (*e.g.* possibly between the head domains) were also involved. The estimated equilibrium dissociation constant for peptide 330–369 (4.3×10^{-9} M) is comparable to the value obtained for *Drosophila* K401 ($\sim 4 \times 10^{-8}$ M) based upon equilibrium sedimentation studies (43). Thus, our data indicate that the dimerization domain located within the neck is sufficiently stable on its own and thus could account for the dimerization observed in these recombinantly expressed motor domain constructs.

In contrast to the mostly helical dimerization domain, our work also indicates that the adjacent COOH-terminal (370–383) and NH_2-terminal (320–332) segments show little helical propensity. The COOH-terminal residues 370–383 contribute little to dimer stability, and we suspect that these residues are part of a flexible hinge that is thought to exist between the neck and the stalk regions. The NH_2-terminal segment of the neck, on the other hand, appears to have the capability of adopting a β-sheet secondary structure. This notion is based upon the finding that deletion of two COOH-terminal heptads from the coiled-coil dimer containing residues 316–369 (K5) causes the residual peptide (316–355) to display a CD spectrum characteristic of a β-sheet at pH 5.5 and to form a gel at neutral pH.

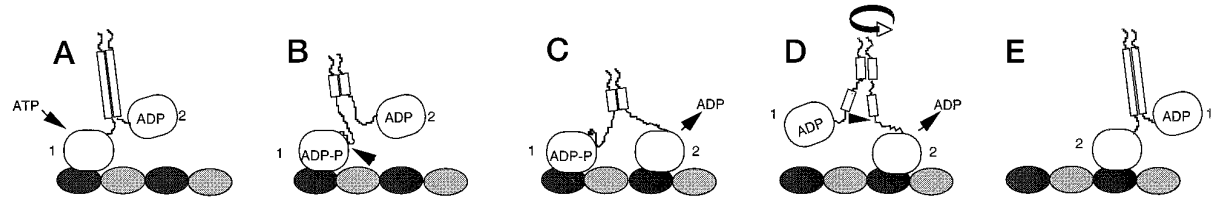

FIG. 9. **Schematic representation of the possible conformational changes occurring in the neck region during kinesin movement.** *Globular spheres* depict the motor domain heads, *rectangular boxes* indicate the kinesin neck region which forms a two-stranded α-helical coiled-coil, and the *shaded ovals* at the base indicate the α and β tubulin subunits. In *step A*, one motor domain head of kinesin is tightly bound to the microtuble filament while the second head (containing ADP) is detached and directed toward the "plus" end of the microtubule, as suggested by cryo-electron microscopy studies. The two heads may be related by ~180° symmetry (57). After hydrolysis of ATP by the bound motor domain, a conformational change is transmitted from the active site to the β linker region (*arrow*, *step B*), which causes the first four heptads of the neck region to unzip. (ADP-P_i is shown in the active site, although this change could equally well occur after phosphate release.) The unzipping of several heptads in the coiled-coil allows the unbound head to now reach the next available tubulin subunit (*steps B–C*). Release of ADP from the newly bound motor domain head to create a tight microtubule binding state coupled with the progression of the other head to a weak microtubule binding state reverses the structural changes in the neck region and enables the coiled-coil dimerization domain to re-zip (*steps C–D*). Coupled to re-zipping, is the rotation of the detached head by 180° (*circular arrow*, Ref. 57). The kinesin enzyme then returns to its initial state (*step E*). For a more detailed description of each step occurring in the model, see "Discussion."

We also observed that the addition of 14 NH_2-terminal residues (316–329) onto the coiled-coil dimerization domain (330–369) caused a net loss of ~8 helical residues without decreasing the stability of the dimeric structure. This would suggest that a nonhelical intermolecular interactions (*e.g.* a small β-sheet secondary structure) can occur in the region between ~325–335. Our observation of β-sheet secondary structure also agrees with a secondary structure predictive algorithm of Holly and Karplus for the NH_2-terminal portion of the neck by Huang *et al.* (6). Since the NH_2-terminal segment appears to be primarily non-helical and connects helix 6 in the crystal structure of the globular motor domain (2) to the helical dimerization domain, we refer to this segment of the neck as the "β linker region."

The β linker region of the neck is of considerable interest, since it appears to play an important role in motility and is highly conserved in many NH_2-terminal motor proteins in the kinesin superfamily. Truncation at *Drosophila* kinesin residue 340 (human kinesin 332) eliminates the dimerization domain, and yet the motor still produces directional movement in a multiple motor microtubule gliding assay (7, 13–15,). Amino acid mutants in the β linker region of the neck also yield kinesin proteins that are severely defective in motility.[2] Whether a structural change occurs in the linker region during the force-generation cycle is unknown. However, the finding that this region can revert to a fully helical structure in the presence of 50% TFE indicates that this region has the intrinsic ability to adopt both β-strand and helical structures depending on the external environment. Thus, one could imagine that the β linker region could undergo a structural transition during the ATPase cycle, as will be discussed below.

Coiled-Coil Interactions within the Dimerization Domain Are Organized in a Strong-Weak-Strong manner—GdnHCl denaturation studies of the kinesin peptides indicate that the coiled-coil dimerization domain is arranged in a strong-weak-strong pattern. Full stability of the dimerization domain is achieved only when all six of the spanning heptads (from residues 330–369) are present. Deletion of two heptads (14 residues) from the COOH terminus (K1 peptide) results in a complete loss of all α-helical content, which is surprising considering that four of the six heptads still remain. Deletion of the two NH_2-terminal heptads (K3 peptide), on the other hand, drastically decreases stability and ellipticity, although a dimeric structure can still be observed by gel filtration. These observations indicate that both the N- and COOH-terminal heptads are important for the stability of the structure, with the COOH-terminal heptads appearing to be the most important. These results agree with those of Corriea *et al.* (43), who showed that truncation of the COOH-terminal 1.5 heptads of the proposed dimerization domain in *Drosophila* kinesin produces a protein (K366) that fails to dimerize at concentrations up to 4 μM.

Interestingly, the central portion of the dimerization domain contains three residues, Tyr^{344}, Glu^{347}, and Asn^{351}, that destabilize the coiled-coil structure. Introducing these amino acids into a model coiled-coil sequence has a significant destabilizing effect, and conversely, substituting these three residues in a kinesin neck peptide with ideal hydrophobic residues increases the stability of the coiled-coil interaction. Residues Tyr^{344} and Glu^{347} are highly conserved among several classes of NH_2-terminal kinesin motors, suggesting that their role in destabilizing the central region of the coiled-coil may serve an important function. It is interesting to note that the Glu^{347} residues within the "hydrophobic" core are surrounded by opposite charged lysine and arginine residues in adjacent *e* and *g* positions (Fig. 8). Glover *et al.* (45) observed in a c-Fos/c-Jun coiled coil crystal structure that a lysine residue located within a core position could potentially form hydrogen bonds and/or electrostatic interaction with adjacent residues in the *e* and *g* positions and speculated that this could stabilize the structure. Therefore the devastating effect of packing glutamic acid residues into the hydrophobic core in the kinesin neck could be mitigated to some extent by the formation of salt bridges with nearby residues. Such electrostatic interactions could possibly explain the higher than expected equilibrium association constant of the K3 peptide, even though it is very unstable in GdnHCl (which disrupts salt bonds).

Another intriguing feature of the model representation of the coiled-coil dimerization domain in Fig. 8 is that the majority of electrostatic interactions across the core (e–g') are repulsive (indicated by the *arrows* in Fig. 8). Previous studies with model coiled-coil sequences have shown that attractive electrostatic interactions can be used to increase coiled-coil stability, control dimer orientation (parallel *versus* antiparallel), and govern homo- *versus* heterodimerization (27, 29, 35, 36, 40, 46, 47) (for recent reviews, see also Refs. 48–52). The lack of significant attractive electrostatic interactions, taken together with our data showing an instability within the hydrophobic core, may indicate that the stability of the neck domain is optimized not only for its structure but also for its function as discussed below.

A Model for Kinesin Motility Involving Structural Transitions within the Neck Region—Studies on the kinesin dimer have indicated that the enzymatic cycles of the two kinesin motor domains may be coupled during processive movement. The strongest evidence for this idea comes from Hackney (55), who showed that a kinesin dimer containing two bound ADP

molecules releases ADP rapidly from one site and slowly from a second site after mixing with microtubules in a nucleotide-free buffer. Since microtubule interaction stimulates ADP release, Hackney suggested that after one head bound to the microtubule, the partner head had restricted access to a microtubule binding site. This idea is also consistent with recent cryo-EM images of microtubules decorated with dimeric kinesin, which show one kinesin head bound to the microtubule and the second head detached and oriented toward the plus-end of the microtubule (53, 54). Hackney (55) and Ma and Taylor (56) have also shown that ATP binding and hydrolysis by the microtubule-bound kinesin head enables the partner head to bind to the microtubule and release its ADP. These results have led to the suggestion that the two kinesin heads in a dimer are predominantly in different states: one head strongly binds to the microtubule and weakly binds to ADP, while the second head weakly binds to the microtubule and strongly binds to ADP (55, 56). The two heads are suggested to alternate between these two states during processive movement.

Our results on the thermodynamic properties of kinesin neck peptides suggest a model that could provide an explanation for the results described above. The model shown in Fig. 9 begins with one head (without nucleotide) tightly bound to the microtubule, while the second head (containing ADP) is detached and directed toward the microtubule plus-end (Fig. 9, *step A–B*). In this state, the 6 heptad repeats in the neck domain are proposed to exist in a coiled-coil structure, which constrains the detached head from reaching an adjacent microtubule binding site. After the bound head binds and hydrolyzes ATP, a conformational change occurs in the globular motor domain, which is propagated to the nearby neck domain (Fig. 9, *steps B–C*). As a consequence, the β linker region of the neck domain changes its structure or interacts in a new manner with the core motor domain, and thereby acts like a contracting spring. This conformational change would account for the observation that monomeric kinesin containing the β linker region, although not processive, can elicit force and directional movement. In the kinesin dimer, the conformational change in the β linker region results in a loss of α-helical residues at the NH_2 terminus of the coiled-coil dimerization domain. This, in turn, could result in a cooperative unzippering of the majority of the coiled-coil up to the last two stable heptad repeats (since the middle two heptads are inherently unstable). Unwinding of the coiled-coil would create a flexible linker between the heads, which would allow the detached head to reach an adjacent microtubule binding site (*step B–C*). Directional movement to a forward binding site could be favored by the initial positioning of the detached head closer to the plus-end of the microtubule (53, 54). Upon docking to the microtubule, the forward head would then release its ADP and enter a strong microtubule-binding state, while the rearward head would have progressed in the cycle to a weak-binding ADP state (Fig. 9, *steps C–D*). These events would also reverse the structural change in the linker region of the neck, which would permit the coiled-coil in the dimerization domain to "re-zip." In the process, the rearward head would rotate by ~180° (57), returning the enzyme to its initial state in the cycle and thereby completing one mechanical step.

The above model makes several predictions concerning the roles of different regions within the neck domain. Most notably, enhancing the stability of the middle heptad repeats in the dimerization domain should impair processivity and alternating head ATP catalysis as a result of increasing the energetic requirement for unraveling the coiled-coil as a prelude to separating the heads. Experiments are currently under way to examine this question.

Acknowledgments—We thank Lorne Burke, Paul Semchuck, and Kim Oikawa for technical assistance in peptide synthesis, purification, and CD spectroscopy. We also are grateful to C. T. Mant, C. Coppin, and L. Romberg for helpful discussions and comments on this manuscript. We also thank Drs. T. Shimizu and H. Morii for sharing their unpublished data on kinesin neck region peptides during the course of this work.

REFERENCES

1. Vale, R. D. (1993) in *Guidebook to the Cytoskeletal and Motor Proteins* (Kreis, T., and Vale, R., eds) pp. 175–183, Oxford University Press, Oxford
2. Kull, F. J., Sablin, E. P., Lau, R., Fletterick, R. J., and Vale, R. D. (1996) *Nature* **380,** 550–555
3. Sablin, E. P., Kull, F. J., Cooke, R., Vale, R. D., and Fletterick, R. J. (1996) *Nature* **380,** 555–559
4. Bloom, G. S., Wagner, M. C., Pfister, K. K., and Brady, S. T. (1988) *Biochemistry* **27,** 3409- 3416
5. Kuznetsov, S. A., Vaisberg, E. A., Shanina, N. A., Magretova, N. N., Chernyak, V. Y., and Gelfand, V. I. (1988) *EMBO J.* **7,** 353–356
6. Huang, T.-G., Suhan, J., and Hackney, D. D. (1994) *J. Biol. Chem.* **269,** 16502–16507
7. Stewart, R. J., Thaler, J. P., and Glodstein, L. S. B. (1993) *Proc. Natl. Acad. Sci. U. S. A.* **90,** 5209–5213
8. Hirokawa, N., Pfister, K. K., Yorifuji, H., Wagner, M. C., Brady, S. T., and Bloom, G. S. (1989) *Cell* **56,** 867–878
9. Scholey, J. M., Heuser, J., Yang, J. T., and Goldstein, L. S. B. (1989) *Nature* **338,** 355–357
10. Yang, J. T., Laymon, R. A., and Goldstein, L. S. B. (1989) *Cell* **56,** 879–889
11. de Cuevas, M., Tao, T., and Goldstein, L. S. B. (1992) *J. Cell Biol.* **116,** 957–965
12. Svoboda, K., Schmidt, C. F., Schnapp, B. J., and Block, S. M. (1993) *Nature* **365,** 721–727
13. Yang, J. T., Saxton, W. M., Stewart, R. J., Raff, E. C., and Goldstein, L. S. (1990) *Science* **249,** 42–47
14. Vale, R. D., Funatsu, T., Pierce, D. W., Romberg, L., Harada, Y., and Yanagida, T. (1996) *Nature* **380,** 451–453
15. Berliner, E., Young, E. C., Anderson, K., Mahtani, H. K., and Gelles, J. (1995) *Nature* **373,** 718–721
16. Hackney, D. D. (1995) *Nature* **377,** 448–450
17. Sereda, T. J., Mant, C. T., Quinn, A. M., and Hodges, R. S. (1993) *J. Chromatogr.* **646,** 17–30
18. Pace, C. N. (1986) *Methods Enzymol.* **131,** 266–279
19. Shortle, D. (1989) *J. Biol. Chem.* **264,** 5315–5318
20. De Francesco, R., Pastore, A., Vecchio, G., and Cortese, R. (1991) *Biochemistry* **30,** 143–147
21. Farrow, N. A., Muhandiram, R., Singer, A. U., Pascal, S. M., Kay, C. M., Gish, G., Shoelsen, S. E., Pawson, T., Forman-Kay, J. D., and Kay, L. E. (1994) *Biochemistry* **33,** 5984–6003
22. Monera, O. D., Sereda, T. J., Zhou, N. E., Kay, C. M., and Hodges, R. S. (1995) *J. Pept. Sci.* **1,** 319–392
23. Chen, Y. H., Yang, J. T., and Martinez, H. M. (1972) *Biochemistry* **11,** 4120–4131
24. Gans, P. L., Lyu, P. C., Manning, M. C., Woody, R. W., and Kallenbach, N. R. (1991) *Biopolymers* **31,** 1605–1614
25. Engel, M., Williams, R. W., and Erickson, B. W. (1991) *Biochemistry* **30,** 3161–3169
26. Lau, S. Y. M., Taneja, A. K., and Hodges, R. S. (1984) *J. Chromatogr.* **317,** 129–140
27. Monera, O. D., Zhou, N. E., Kay, C. M., and Hodges, R. S. (1993) *J. Biol. Chem.* **268,** 19218–19227
28. Zhou, N. E., Kay, C. M., and Hodges, R. S. (1992) *Biochemistry* **31,** 5739–5746
29. Zhou, N. E., Zhu, B. Y., Kay, C. M., and Hodges, R. S. (1992) *Biopolymers* **32,** 419–426
30. Zhu, B. Y., Zhou, N. E., Semchuk, P. D., Kay, C. M., and Hodges, R. S. (1992) *Int. J. Pept. Protein Res.* **40,** 171–179
31. Sonnichsen, F. D., Van Eyk, J. E., Hodges, R. S., and Sykes, B. D. (1992) *Biochemistry* **31,** 8790–8798
32. Zhou, N. E., Kay, C. M., and Hodges, R. S. (1992) *J. Biol. Chem.* **267,** 2664–2670
33. Zhou, N. E., Kay, C. M., and Hodges, R. S. (1993) *Biochemistry* **32,** 3178–3187
34. Graddis, T. J., Myszka, D. G., and Chaiken, I. M. (1993) *Biochemistry* **32,** 12664–12671
35. Kohn, W. D., Kay, C. M., and Hodges, R. S. (1995) *Protein Sci.* **4,** 237–250
36. Kohn, W. D., Monera, O. D., Kay, C. M., and Hodges, R. S. (1995) *J. Biol. Chem.* **270,** 25495–25506
37. O'Shea, E. K., Klemm, J. D., Kim, P. S., and Alber, T. (1991) *Science* **254,** 539–544
38. Schuermann, M., Hunter, J. B., Hennig, G., and Muller, R. (1991) *Nucleic Acids Res.* **19,** 739–746
39. Su, J. Y., Hodges, R. S., and Kay, C. M. (1994) *Biochemistry* **33,** 15501–15510
40. Zhu, B. Y., Zhou, N. E., Kay, C. M., and Hodges, R. S. (1993) *Protein Sci.* **2,** 383–394
41. Holley, L. H., and Karplus, M. (1989) *Proc. Natl. Acad. Sci. U. S. A.* **86,** 152–156
42. Lupas, A., Dyke, M. V., and Stock, J. (1991) *Science* **252,** 1162–1164
43. Correia, J. J., Gilbert, S. P, Moyer, M. L., and Johnson, K. A. (1995) *Biochemistry* **34,** 4898–4907
44. Morii, H., Takenawa, T., Arisaka, F., and Shimizu, T. (1997) *Biochemistry*, in press
45. Glover, J. N. M., and Harrison, S. C. (1995) *Nature* **373,** 257–261
46. Monera, O. D., Kay, C. M., and Hodges, R. S. (1994) *Biochemistry* **33,** 3862–3871

47. Zhou, N. E., Kay, C. M., and Hodges, R. S. (1994) *J. Mol. Biol.* **237,** 500–512
48. Adamson, J. G., Zhou, N. E., and Hodges, R. S. (1993) *Curr. Opin. Biotechnol.* **4,** 428–437
49. Alber, T. (1992) *Curr. Opin. Genet. Dev.* **2,** 205–210
50. Baxevanis, A. D., and Vinson, C. R. (1993) *Curr. Opin. Genet. Dev.* **3,** 278–285
51. Hodges, R. S. (1992) *Curr. Biol.* **2,** 122–124
52. Hodges, R. S. (1996) *Biochem. Cell Biol.* **74,** 133–154
53. Arnal, I., Metoz, F., DeBonis, S., and Wade, R. H. (1996) *Curr. Biol.* **6,** 1265–1270
54. Hirose, K., Lockhart, A., Cross, R. A., and Amos, L. A. (1996) *Proc. Natl. Acad. Sci. U. S. A.* **93,** 9539–9544
55. Hackney, D. D. (1994) *Proc. Natl. Acad. Sci. U. S. A.* **91,** 6865–6869
56. Ma, Y.-Z., and Taylor, E. W. (1997) *J. Biol. Chem.* **272,** 724–730
57. Howard, J. (1996) *Annu. Rev. Physiol.* **58,** 703–729
58. Chen, Y. H., Yang, J. T., and Chau, K. H. (1974) *Biochemistry* **13,** 3350–3359